Contribution from the Department of Chemistry and Biochemical Sciences, Oregon Graduate Center, Beaverton, Oregon 97006, and Department of Chemistry, Colorado State University, Fort Collins, Colorado 80523

Crystal and Molecular Structure of the (μ-Oxo)bis[aquobis(phenanthroline)iron(III)] Complex, a Raman Spectroscopic Model for the Binuclear Iron Site in Hemerythrin and Ribonucleotide Reductase

JEFFREY E. PLOWMAN,[1] THOMAS M. LOEHR,*[2a] CYNTHIA K. SCHAUER,[2b] and OREN P. ANDERSON[2b]

The crystal structure of the binuclear iron complex [Fe$_2$O(phenanthroline)$_4$(H$_2$O)$_2$](NO$_3$)$_4$·5H$_2$O has been investigated. This compound crystallizes in the triclinic system, space group $P\bar{1}$, with a = 13.828 (2) Å, b = 15.122 (2) Å, c = 15.890 (2) Å, α = 84.44 (1)°, β = 64.99 (1)°, γ = 68.46 (1)°, and Z = 2. The dimeric cation exhibits typical Fe–μ-O bond lengths of 1.785 Å and a bridge angle of 155.1°. Infrared and Raman spectroscopic methods have been used to study the symmetric and asymmetric Fe–O–Fe vibrational modes. ν_s(Fe–O–Fe) was observed at 395 cm^{-1} in the Raman spectrum and found to shift ~5 cm^{-1} upon ^{18}O exchange. The intensity of this mode is strongly dependent upon excitation wavelength and exhibits an enhancement maximum at ~380 nm. This value lies within a region of increasing absorbance in the near-ultraviolet region and is assigned to an O^{2-} → Fe(III) charge-transfer transition. The asymmetric vibration for the Fe–O–Fe cluster was observed at 827 cm^{-1} in both the IR and Raman spectra and was found to shift ~40 cm^{-1} to lower energy upon ^{18}O substitution. The μ-oxo-bridged iron complex is, thus, a good model for the vibrational spectroscopic properties of the binuclear iron proteins hemerythrin and ribonucleotide reductase.

Introduction

Complex formation between iron and 1,10-phenanthroline was first described by Blau[3] in the 1890s. Nearly 40 years later, Gaines et al.[4] noted the anomalously low magnetic moment (~1.4 μ$_B$/Fe) of a compound corresponding to a phenanthroline:Fe stoichiometry of 2:1, which was rationalized by proposing the existence of a binuclear iron complex having two hydroxide ion bridges, [(phen)$_2$FeOH]$_2^{4+}$. Further magnetic and infrared absorption studies on several phenanthroline complexes led Khedekar et al. to reformulate these compounds as μ-oxo-bridged binuclear iron species.[5] All of these complexes show antiferromagnetic coupling with $-J \approx$ 100 cm^{-1} and a strong band and in the IR spectrum between 820 and 840 cm^{-1}, which is characteristic of an asymmetric Fe–O–Fe vibrational mode.[5] The present study was undertaken to provide X-ray crystallographic verification for the presence of a μ-oxo bridge in these complexes and to investigate their infrared, Raman, and electronic absorption properties as models for the μ-oxo-bridged binuclear iron proteins.

The two proteins that are known to fit into this category are hemerythrin, a respiratory protein in marine invertebrates,[6,7] and ribonucleotide reductase, an enzyme that catalyzes the formation of deoxyribonucleotide precursors for DNA biosynthesis.[8,9] Definitive evidence for a μ-oxo bridge in the binuclear iron center of hemerythrin has been provided by X-ray crystallography,[10–12] X-ray absorption spectroscopy,[13,14] electronic spectroscopy,[15–17] resonance Raman spectrosco-

py,[18–20] and magnetic susceptibility measurements.[21,22] Although X-ray data are lacking for ribonucleotide reductase, it is similar to hemerythrin in its electronic and Mössbauer spectra and in the strong antiferromagnetic coupling ($-J$ = 108 cm^{-1}) between the two iron atoms.[23,24] Both proteins show a resonance-enhanced vibrational mode at ~500 cm^{-1} in their Raman spectra, which is at the expected frequency for the symmetric vibration of a bent Fe–O–Fe cluster. The ~15-cm^{-1} shift to lower frequency that occurs when either of the proteins is prepared in H$_2$^{18}O verifies the presence of a solvent-derived μ-oxo-bridge oxygen.[18–20,25] Since resonance Raman spectroscopy offers one of the most direct means for identifying this common structural feature in proteins, it is of interest to examine the Raman spectra of μ-oxo-bridged Fe(III) model complexes.

Strong resonance-enhancement of Raman-active ν_s(M–O–M) has been observed for the oxo-bridged dimers Fe$_2$O(TPP)$_2$, (Os$_2$OCl$_{10}$)$^{4-}$, (Ru$_2$OCl$_{10}$)$^{4-}$, and (Re$_2$OCl$_{10}$)$^{4-}$ upon excitation within their visible absorption bands.[26–28] However, Solbrig et al. in a study of eight oxo-bridged Fe(III) dimer complexes with carboxylate and Schiff base ligand sets were unable to locate any O-isotope-sensitive Fe–O–Fe modes using visible light excitation.[29] They did locate an isotope-sensitive ν_s-(Fe–O–Fe) at 458 cm^{-1} and ν_{as}(Fe–O–Fe) at 870 cm^{-1} in the Raman spectrum (not resonance enhanced) of the [Fe$_2$OCl$_6$]$^{2-}$

(1) Present address: Chemistry Division, DSIR, Fendalton, Christchurch, New Zealand.
(2) (a) Oregon Graduate Center. (b) Colorado State University.
(3) Blau, F. *Monatsh. Chem.* **1898**, *19*, 647.
(4) Gaines, A., Jr.; Hammett, L. P.; Walden, G. H., Jr. *J. Am. Chem. Soc.* **1936**, *58*, 1668.
(5) Khedekar, A. V.; Lewis, J.; Mabbs, F. E.; Weigold, H. *J. Chem. Soc. A* **1967**, 1561.
(6) Wilkins, R. G.; Harrington, P. C. *Adv. Inorg. Biochem.* **1983**, *5*, 51.
(7) Sanders-Loehr, J.; Loehr, T. M. *Adv. Inorg. Biochem.* **1979**, *1*, 235.
(8) Sjöberg, B.-M.; Gräslund, A. *Adv. Inorg. Biochem.* **1983**, *5*, 87.
(9) Reichard, P.; Ehrenberg, A. *Science (Washington, D.C.)* **1983**, *221*, 514.
(10) Stenkamp, R. E.; Sieker, L. C.; Jensen, L. H. *J. Am. Chem. Soc.* **1984**, *106*, 618.
(11) Stenkamp, R. E.; Sieker, L. C.; Jensen, L. H.; Sanders-Loehr, J. *Nature (London)* **1981**, *291*, 263.
(12) Hendrickson, W. A. In "Invertebrate Oxygen Binding Proteins: Structure, Active Site, and Function"; Lamy, J., Lamy, J., Eds.; Marcel-Dekker: New York, 1981; p 503.
(13) Elam, W. T.; Stern, E. A.; McCallum, J. D.; Sanders-Loehr, J. *J. Am. Chem. Soc.* **1982**, *104*, 6369.
(14) Hendrickson, W. A.; Co, M. S.; Smith, J. L.; Hodgson, K. O.; Klippenstein, G. L. *Proc. Natl. Acad. Sci. U.S.A.* **1982**, *79*, 6255.
(15) Garbett, K.; Darnall, D. W.; Klotz, I. M.; Williams, R. J. P. *Arch. Biochem. Biophys.* **1969**, *135*, 419.

(16) Gray, H. B.; Schugar, H. J. In "Inorganic Biochemistry"; Eichhorn, G. L., Ed.; Elsevier: Amsterdam, 1973; p 102.
(17) Sanders-Loehr, J.; Loehr, T. M.; Mauk, A. G.; Gray, H. B. *J. Am. Chem. Soc.* **1980**, *102*, 6992.
(18) Kurtz, D. M., Jr.; Shriver, D. F.; Klotz, I. M. *Coord. Chem. Rev.* **1977**, *24*, 145.
(19) Freier, S. M.; Duff, L. L.; Shriver, D. F.; Klotz, I. M. *Arch. Biochem. Biophys.* **1980**, *205*, 449.
(20) Shiemke, A. K.; Loehr, T. M.; Sanders-Loehr, J. *J. Am. Chem. Soc.* **1984**, *106*, 4951.
(21) Dawson, J. W.; Gray, H. B.; Hoenig, H. E.; Rossman, G. R.; Schredder, J. M.; Wang, R.-H. *Biochemistry* **1972**, *11*, 461.
(22) Moss, T. H.; Moleski, C.; York, J. L. *Biochemistry* **1971**, *10*, 840.
(23) Atkin, C. L.; Thelander, L.; Reichard, P.; Lang, G. *J. Biol. Chem.* **1973**, *248*, 7464.
(24) Peterson, L.; Gräslund, A.; Ehrenberg, A.; Sjöberg, B.-M.; Reichard, P. *J. Biol. Chem.* **1980**, *255*, 6706.
(25) Sjöberg, B.-M.; Loehr, T. M.; Sanders-Loehr, J. *Biochemistry* **1982**, *21*, 96.
(26) Burke, J. J.; Kincaid, J. R.; Spiro, T. G. *J. Am. Chem. Soc.* **1978**, *100*, 6077.
(27) San Filippo, J., Jr.; Grayson, R. L.; Sniadoch, H. J. *Inorg. Chem.* **1976**, *15*, 269.
(28) Campbell, J. R.; Clark, R. J. H. *J. Chem. Soc., Faraday Trans. 2* **1980**, *76*, 1103.
(29) Solbrig, R. M.; Duff, L. L.; Shriver, D. F.; Klotz, I. M. *J. Inorg. Biochem.* **1982**, *17*, 69.

complex.[29] In the Raman spectra of the $[Fe_2O(phen)_4$-$(H_2O)_2]^{4+}$ complexes reported here, we have been able to observe both the symmetric and the asymmetric Fe–O–Fe vibrations. The ν_s(Fe–O–Fe) is maximally enhanced by excitation within the near-ultraviolet absorption envelope. Similarly, ν_s and ν_{as} in hemerythrin and ν_s in ribonucleotide reductase also reach their highest intensity with near-ultraviolet excitation.[20,25]

Experimental Section

Reagent grade $NaClO_4$ and 1,10-phenanthroline (phen) (Aldrich), $Fe(NO_3)_3 \cdot 9H_2O$, $FeCl_3 \cdot 6H_2O$, and $Fe(ClO_4) \cdot 6H_2O$ (Alfa Inorganics), and $FeSO_4 \cdot 7H_2O$ (Mallinckrodt) were used without further purification. [^{18}O]Water (96–99%) was obtained from the Monsanto Research Corp. Analyses were performed by Galbraith Laboratories, Knoxville, TN.

$Fe(phen)_3(ClO_4)_3 \cdot 3H_2O$. The method of Burstall and Nyholm[30] for the 2,2'-bipyridyl complex was adopted for the preparation of this compound. $FeSO_4 \cdot 7H_2O$ (1.0 g) in distilled water (70 mL) was treated with concentrated H_2SO_4 (0.2 mL) and phen (2.14 g) and the blood red solution filtered. The solution was cooled to 4 °C in an ice bath and saturated with Cl_2 gas, generated by adding concentrated HCl to $KMnO_4$. On warming to room temperature, the solution developed a deep blue color, and more Cl_2 was passed through to ensure complete oxidation. An excess of 30% $NaClO_4$ solution was added, whereupon a blue precipitate formed. The solid was filtered out, washed well with water, and dried in air.

Anal. Calcd for $C_{36}H_{24}N_6O_{12}Cl_3Fe \cdot 3H_2O$: C, 45.57; H, 3.19; N, 8.86; Cl, 11.21; Fe, 5.89. Found: C, 46.34; H, 2.99; N, 8.47; Cl, 10.79; Fe, 5.60.

$[Fe_2O(phen)_4(H_2O)_2]X_4$ Complexes. The general methods described by Gaines et al.[4] and Khedekar et al.[5] were adopted in the preparation of these complexes. One millimole of either $FeCl_3 \cdot 6H_2O$, $Fe(NO_3)_3 \cdot 9H_2O$, or $Fe(ClO_4)_3 \cdot 6H_2O$, dissolved in 10 mL of water, was added to a slurry of 2 mmol of phen in 10 mL of water. A deep red color developed as the phen dissolved, and when this was complete, the reaction mixtures were set aside in the dark to allow crystallization to occur. Since not all of the phen dissolved in the preparation of the perchlorate complex, it was necessary to filter this solution. Crystallization of the chloride and perchlorate salts occurred over night; the nitrate salt was much more soluble, and the first crystals appeared after about 3 weeks. The crystals were filtered out and air-dried.

Anal. Calcd for chloride salt, $C_{48}H_{32}N_8OCl_4Fe_2 \cdot 6H_2O$: C, 52.49; H, 4.04; N, 10.20; Fe, 10.17. Found: C, 52.64; H, 4.06; N, 10.28; Fe, 9.95. Calcd for nitrate salt, $C_{48}H_{32}N_{12}O_{13}Fe_2 \cdot 7H_2O$: C, 47.15; H, 3.79; N, 13.75; Fe, 9.14. Found: C, 48.28; H, 3.37; N, 14.07; Fe, 8.99. Calcd for perchlorate salt, $C_{48}H_{32}N_8O_{17}Cl_4Fe_2 \cdot 6H_2O$: C, 42.57; H, 3.27; N, 8.27; Fe, 8.25. Found: C, 42.04; H, 3.61; N, 8.59; Fe, 8.32.

Crystals suitable for X-ray crystallographic studies were prepared as above; however, at the first sign of precipitation the solutions were filtered and the filtrates were placed in beakers sealed with Parafilm. Crystals usually appeared after 2–3 weeks. The nitrate salt gave rise to the best crystals because of its slower crystallization, and these were selected for the X-ray diffraction analysis.

The ^{18}O-substituted complexes were prepared in a manner similar to the preparation of their ^{16}O analogues except that the solutions were 2–5 times more concentrated. $FeCl_3 \cdot 6H_2O$ (0.2 mmol) was dissolved in 1 mL of $H_2^{18}O$, and to this solution was added 0.4 mmol of phen. For the nitrate salt, 1 mmol of phen was added to 0.5 mmol of $Fe(NO_3)_3 \cdot 9H_2O$ dissolved in 1 mL of $H_2^{18}O$. After the phen had dissolved, the solutions were left to stand. Crystallization of both complexes occurred within 30 min.

Anal. Calcd for the chloride salt, $C_{48}H_{32}N_8^{18}OCl_4Fe_2 \cdot 6H_2^{18}O$: C, 51.83; H, 3.99; N, 10.07; Fe, 10.04. Found: C, 50.79; H, 4.29; N, 9.76; Fe, 9.69. Calcd for the nitrate salt, $C_{48}H_{32}N_{12}^{16}O_{12}^{18}OFe_2 \cdot 7H_2^{18}O$: C, 46.54; H, 3.74; N, 13.57; Fe, 9.02. Found: C, 46.94; H, 3.94; N, 13.64; Fe, 8.16.

Instrumentation. Electronic spectra were recorded on a Cary 16 spectrophotometer, and IR spectra, on a Perkin-Elmer 621 grating spectrophotometer. Raman spectra were obtained on an automated Jarrell-Ash 25-300 Raman spectrophotometer[31] using Spectra-Physics

164 Ar and Kr ion lasers and an RCA C31034 photomultiplier with photon-counting electronics. Raman spectra were obtained on samples held in glass capillaries and cooled to $\sim$77 K in a cold-finger Dewar[25] or in a spinning sample holder at room temperature. Sample deterioration was minimal in both instances, although generally higher quality data were obtained at the low temperatures.

X-ray Structure Determination. The crystal structural data were collected on a Nicolet R3m/E X-ray diffractometer using graphite-monochromatized Mo Kα radiation ($\lambda = 0.71073$ Å). No absorption correction was applied during data reduction[32] because of the small size of the crystal ($0.29 \times 0.23 \times 0.36$ mm) and its low absorption coefficient ($\mu = 5.99$ cm^{-1}). The intensities of 9097 reflections with $3.5° < 2\theta < 50.0°$ were examined by $\theta/2\theta$ scans on the diffractometer. A total of 5613 unique reflections were accepted as observed [$F > 2.5\sigma(F)$] after data reduction (Lorentz and polarization corrections) and were used in the structure refinement.

$[Fe_2O(phen)_4(H_2O)_2](NO_3)_4 \cdot 5H_2O$ (fw 1222.65) crystallizes in space group $P\bar{1}$ ($Z = 2$)[33] with $a = 13.828$ (2) Å, $b = 15.122$ (2) Å, $c = 15.890$ (2) Å, $\alpha = 84.44$ (1)°, $\beta = 64.99$ (1)°, $\gamma = 68.46$ (1)°, $V = 2893.6$ Å^3, and $\rho_{calcd} = 1.40$ g cm^{-3} at -130 °C. Mean values of $|E^2 - 1|$ provided a strong indication that the centrosymmetric space group was the appropriate choice (rather than $P1$). Two iron atoms were located from the Patterson map, and subsequent Fourier syntheses readily revealed all ligand atoms, together with two of the four nitrate groups. After preliminary least-squares refinement[32] of positional and isotropic thermal parameters for these atoms, examination of a difference Fourier map led to the conclusion that the remaining two nitrate ions and the five water molecules of hydration were severely disordered. To represent these disordered species during refinement, site occupancy factors less than 1.0 were employed for rigid, idealized nitrate ions (N–O = 1.24 Å, O–N–O = 120°) and single oxygen atoms (water molecules). Such species were placed at all reasonable positions corresponding to peaks with height greater than 1.0 e Å^{-3} in the electron density map. During refinement, site occupancy factors for these groups were adjusted to sum to the established chemical formula.[5]

Final refinement calculations included anisotropic thermal parameters for all non-hydrogen atoms of the $[Fe_2O(phen)_4(H_2O)_2]^{4+}$ unit and isotropic thermal parameters for the remaining atoms. Hydrogen atoms of the phenanthroline ligands were placed in calculated, idealized positions. At convergence (average shift/esd < 1%), $R = 0.0895$, $R_w = 0.0919$, and the standard deviation in an observation of unit weight was 2.65. These rather unsatisfactory residual indices undoubtedly owe their relatively high values to unresolved difficulties in modeling the disordered electron density within the lattice. In a final difference Fourier map, the maximum peak observed had a height of 1.02 e Å^{-3} and was in the immediate vicinity of one of the most severely disordered nitrate groups.

Table I consists of a list of the atomic coordinates and isotropic thermal parameters for all non-hydrogen atoms of this structure. Table II contains selected bond lengths, and Table III contains a listing of bond angles associated with the structure of the complex cation. Other tables have been included as supplementary material (Table SI—anisotropic thermal parameters, Table SII—calculated coordinates and U's for hydrogen atoms, Table SIII—metric parameters for unconstrained nitrate groups, Table SIV—site occupancy factors, and Table SV—structure factors).

Results and Discussion

The structure of the $[Fe_2O(phen)_4(H_2O)_2]^{4+}$ cation is displayed in Figure 1. As expected from spectroscopic results, the two ferric iron atoms are bridged by a single oxo ligand. The remaining ligand atoms complete a distorted-octahedral ligand array about each iron atom, with the aquo ligand cis to the bridging oxo atom in each case. The Fe–O–Fe linkage is distinctly nonlinear, exhibiting an angle (Fe1–O–Fe2) of 155.1 (4)°. This value is intermediate in the range of Fe–O–Fe angles (139–180°) known from previous studies.[34] The Fe–

(30) Burstall, F. H.; Nyholm, R. S. *J. Chem. Soc.* **1952**, 3570.
(31) Loehr, T. M.; Keyes, W. E.; Pincus, P. A. *Anal. Biochem.* **1979**, *96*, 456.

(32) All crystallographic computations were carried out with use of the SHELXTL program package written by G. M. Sheldrick and supplied by Nicolet XRD for the Data General Eclipse S/140 computer in the crystallography laboratory at Colorado State University.
(33) "International Tables for X-Ray Crystallography"; Kynoch Press: Birmingham, England, 1969; Vol. I.
(34) Thich, J. A.; Toby, B. H.; Powers, D. A.; Potenza, J. A.; Schugar, H. J. *Inorg. Chem.* **1981**, *20*, 3314.

Table I. Atomic Coordinates (×10^4) and Isotropic Thermal Parameters (A^2 × 10^3)

atom	x	y	z	U_{iso}	atom	x	y	z	U_{iso}
Fe1	3559 (1)	2570 (1)	1723 (1)	38 (1)^a	C45	1175 (10)	−1256 (8)	5185 (12)	92 (8)^a
Fe2	2193 (1)	1893 (1)	3945 (1)	39 (1)^a	C46	1857 (9)	−1122 (7)	3448 (10)	89 (7)^a
μ-O	2631 (4)	2235 (4)	2775 (4)	39 (3)^a	C47	2205 (9)	−598 (7)	2704 (10)	89 (7)^a
H$_2$O1	3288 (6)	1891 (4)	852 (4)	59 (4)^a	C48	2313 (8)	266 (7)	2832 (8)	65 (6)^a
H$_2$O2	525 (5)	2742 (4)	4399 (4)	46 (3)^a	C49	1700 (7)	82 (6)	4414 (8)	57 (5)^a
N1	4272 (6)	3178 (4)	2381 (4)	38 (3)^a	C410	1424 (7)	465 (7)	5313 (8)	57 (5)^a
N2	5152 (5)	1461 (4)	1491 (5)	42 (3)^a	C411	1015 (9)	−58 (8)	6057 (7)	73 (6)^a
N3	4566 (6)	3153 (5)	419 (5)	43 (4)^a	C412	1583 (8)	−779 (7)	4311 (9)	75 (6)^a
N4	2380 (6)	3941 (5)	1697 (5)	42 (3)^a	N9	1417 (7)	6267 (5)	3521 (5)	49 (4)^a
N5	2508 (6)	2849 (5)	4613 (5)	41 (3)^a	N10	5296 (13)	8346 (10)	1479 (10)	108 (9)^a
N6	3907 (5)	1084 (5)	3884 (5)	45 (3)^a	N11	841 (15)	1526 (13)	1405 (13)	50 (5)
N7	1594 (6)	1289 (5)	5345 (5)	49 (4)^a	N12	6626 (13)	3896 (11)	4814 (11)	36 (4)
N8	2054 (6)	592 (5)	3676 (5)	51 (4)^a	N13	8097 (1)	3497 (8)	4159 (1)	70 (6)
C11	3793 (7)	4023 (6)	2847 (5)	45 (4)^a	N14	7762 (11)	7566 (9)	2340 (9)	115 (5)
C12	4361 (9)	4343 (7)	3220 (6)	55 (6)^a	N15	8893 (11)	4743 (10)	1136 (10)	221 (13)
C13	5438 (9)	3767 (7)	3115 (7)	56 (6)^a	N16	8006 (14)	5462 (12)	1365 (15)	114 (13)
C14	7098 (9)	2252 (8)	2476 (7)	66 (6)^a	O1	1122 (6)	5604 (4)	3958 (4)	63 (4)^a
C15	7550 (8)	1398 (7)	2009 (7)	67 (6)^a	O2	827 (5)	7115 (4)	3871 (4)	58 (3)^a
C16	7327 (9)	178 (7)	1200 (7)	70 (5)^a	O3	2240 (6)	6122 (5)	2783 (5)	79 (4)^a
C17	6659 (9)	−65 (7)	911 (8)	73 (6)^a	O4	6258 (9)	7692 (7)	911 (6)	109 (6)^a
C18	5542 (8)	609 (7)	1081 (7)	60 (5)^a	O5	4973 (10)	8307 (7)	2377 (7)	105 (7)^a
C19	5830 (7)	1689 (6)	1795 (6)	44 (4)^a	O6	4783 (8)	8906 (7)	1051 (8)	97 (6)^a
C110	5355 (7)	2610 (6)	2276 (6)	40 (4)^a	O7	1203 (25)	2126 (20)	1171 (19)	153 (10)
C111	5970 (8)	2879 (7)	2629 (6)	48 (5)^a	O8	1466 (19)	770 (16)	1129 (15)	112 (7)
C112	6907 (8)	1091 (6)	1667 (7)	58 (5)^a	O9	−224 (14)	1716 (12)	1762 (11)	69 (5)
C21	5638 (8)	2729 (7)	−207 (6)	57 (5)^a	O10	7312 (4)	3769 (6)	3897 (5)	87 (3)
C22	6135 (9)	3173 (8)	−1011 (7)	69 (6)^a	O11	5573 (14)	4490 (11)	5037 (11)	69 (5)
C23	5509 (9)	4053 (8)	−1171 (7)	67 (6)^a	O12	7064 (16)	3540 (13)	5304 (13)	83 (6)
C24	3661 (11)	5440 (8)	−613 (8)	78 (7)^a	O13	9732 (18)	4699 (19)	396 (16)	83 (14)
C25	2604 (12)	5827 (7)	−13 (8)	79 (7)^a	O14	8914 (21)	4045 (13)	1617 (16)	51 (9)
C26	933 (9)	5724 (7)	1510 (7)	64 (6)^a	O15	9770 (12)	4025 (10)	974 (13)	25 (5)
C27	561 (8)	5197 (7)	2249 (7)	63 (5)^a	O16	7865 (7)	3517 (11)	5002 (1)	68 (5)
C28	1314 (8)	4307 (7)	2326 (6)	53 (5)^a	O17	9101 (13)	3312 (13)	3579 (4)	79 (6)
C29	2777 (7)	4459 (6)	946 (6)	43 (4)^a	O18	7931 (18)	7983 (16)	1609 (12)	116 (9)
C210	3936 (8)	4028 (6)	286 (6)	46 (5)^a	O19	6775 (13)	7627 (21)	2879 (16)	167 (14)
C211	4379 (9)	4520 (7)	−525 (7)	61 (6)^a	O20	8587 (15)	7017 (17)	2489 (16)	131 (10)
C212	2079 (9)	5363 (6)	832 (6)	54 (5)^a	O21	7150 (20)	5489 (27)	2084 (27)	129 (25)
C31	1819 (8)	3733 (6)	4960 (6)	48 (5)^a	O22	7945 (29)	6119 (18)	835 (26)	88 (17)
C32	2073 (8)	4295 (7)	5433 (6)	58 (5)^a	O23	8922 (15)	5414 (11)	623 (11)	24 (5)
C33	3057 (9)	3925 (8)	5548 (7)	69 (7)^a	O24	7998 (12)	4804 (14)	1830 (11)	34 (6)
C34	4923 (10)	2552 (10)	5199 (8)	79 (8)^a	H$_2$OA	9593 (12)	3216 (9)	3235 (9)	61 (3)
C35	5629 (10)	1671 (9)	4792 (8)	74 (7)^a	H$_2$OB	367 (13)	9525 (11)	671 (10)	108 (5)
C36	6015 (9)	250 (8)	3916 (7)	72 (6)^a	H$_2$OC	1086 (15)	2002 (13)	1762 (12)	63 (5)
C37	5661 (8)	−228 (8)	3495 (7)	69 (6)^a	H$_2$OD	−118 (18)	7957 (15)	627 (14)	94 (6)
C38	4596 (7)	200 (6)	3475 (7)	55 (5)^a	H$_2$OE	5307 (21)	6297 (17)	2886 (16)	115 (8)
C39	4277 (8)	1539 (6)	4288 (6)	45 (5)^a	H$_2$OF	1341 (39)	8285 (33)	475 (31)	135 (15)
C310	3514 (8)	2480 (7)	4690 (6)	47 (5)^a	H$_2$OG	5728 (20)	4168 (16)	5361 (16)	109 (7)
C311	3846 (8)	2982 (7)	5160 (7)	59 (6)^a	H$_2$OH	3923 (22)	6854 (18)	3250 (17)	102 (8)
C312	5314 (8)	1160 (7)	4340 (7)	58 (5)^a	H$_2$OI	10573 (29)	3921 (24)	433 (24)	50 (9)
C41	1312 (7)	1663 (7)	6178 (7)	60 (5)^a	H$_2$OJ	1276 (27)	1564 (23)	488 (23)	87 (10)
C42	868 (8)	1239 (8)	7009 (7)	73 (6)^a	H$_2$OK	825 (27)	4447 (23)	9758 (22)	32 (8)
C43	746 (8)	370 (8)	6883 (9)	95 (7)^a	H$_2$OL	1649 (22)	8580 (18)	768 (18)	76 (7)
C44	878 (10)	−900 (8)	5975 (10)	81 (7)^a	H$_2$OM	11898 (25)	9122 (21)	905 (20)	105 (9)

^{a} Equivalent isotropic U defined as $^1/_3$ × trace of the orthogonalized $\mathbf{U}_{ij}$ tensor.

μ-O distances seen here (Fe1–μ-O = 1.787 (5) Å, Fe2–μ-O = 1.783 (5) Å) are entirely characteristic of such linkages with a known range of 1.755–1.82 Å.[34] The combination of the nonlinear bridge and the strong Fe–μ-O bonding produces an intermetallic spacing of 3.49 Å.

Earnshaw and Lewis[35] were the first to suggest that the magnetic behavior of the oxo-bridged Fe(III) complexes was due to strong antiferromagnetic coupling between two high-spin ($S = ^5/_2$) iron atoms. The structural results for [Fe$_2$O-(phen)$_4$(H$_2$O)$_2$]$^{4+}$ clearly support this assignment of high-spin character, as the Fe–N bonds cis to the bridging oxygen atom are considerably longer (average Fe–N (cis) = 2.15 Å) than the iron(III)–nitrogen bond lengths in the low-spin [Fe-(phen)$_3$]$^{3+}$ complex (average Fe–N = 1.973 Å).[36] In the

oxo-bridged species [Fe(salen)]$_2$O·CH$_2$Cl$_2$, imino nitrogen atoms occupy basal square-pyramidal coordination sites cis to the μ-oxo ligand at distances of 2.10–2.12 Å from the high-spin iron(III) atoms.[37] The nitrogen atoms (N3 and N7) trans to the μ-oxo ligand are subject to a significant trans influence from that strongly bound bridging group (Fe1–N3 = 2.263 (7) Å, Fe2–N7 = 2.253 (7) Å).

Binding of two bidentate ligands to each iron atom leads to the possibility of Δ and Λ conformations about each metal. The diastereoisomer shown in Figure 1 clearly exists in the (Δ,Δ) configuration, and the inversion center present in the lattice guarantees the presence of an equal amount of the (Λ,Λ) diastereoisomer in the crystals. Two of the chelate rings, phen 1 and phen 3 in Figure 1, are nearly parallel to one another (dihedral angle 3.1°) and have a separation of ~3.45 Å. In

(35) Earnshaw, A.; Lewis, J. *J. Chem. Soc.* **1961**, 396.
(36) Baker, J.; Engelhardt, L. M.; Figgis, B. N.; White, A. H. *J. Chem. Soc., Dalton Trans.* **1975**, 530.

(37) Coggon, P.; McPhail, A. T.; Mabbs, F. E.; McLachlan, V. N. *J. Chem. Soc. A* **1971**, 1014.

Table II. Bond Lengths (Å)

Fe1-μ-O	1.787 (5)	Fe1-H$_2$O1	2.027 (9)
Fe1-N1	2.154 (9)	Fe1-N2	2.127 (6)
Fe1-N3	2.263 (7)	Fe1-N4	2.126 (6)
Fe2-μ-O	1.783 (5)	Fe2-H$_2$O2	2.021 (5)
Fe2-N5	2.135 (9)	Fe2-N6	2.198 (7)
Fe2-N7	2.253 (7)	Fe2-N8	2.145 (8)
N1-C11	1.328 (10)	N1-C110	1.371 (11)
N2-C18	1.316 (12)	N2-C19	1.372 (15)
N3-C21	1.333 (9)	N3-C210	1.346 (10)
N4-C28	1.319 (9)	N4-C29	1.385 (11)
N5-C31	1.327 (10)	N5-C310	1.351 (13)
N6-C38	1.351 (10)	N6-C39	1.330 (16)
N7-C41	1.330 (14)	N7-C410	1.360 (14)
N8-C48	1.327 (15)	N8-C49	1.351 (13)
C11-C12	1.390 (19)	C12-C13	1.367 (15)
C13-C111	1.392 (14)	C14-C15	1.345 (15)
C14-C111	1.424 (14)	C15-C112	1.437 (19)
C16-C17	1.356 (22)	C16-C112	1.428 (15)
C17-C18	1.429 (14)	C19-C110	1.437 (12)
C19-C112	1.367 (12)	C110-C111	1.380 (18)
C21-C22	1.409 (14)	C22-C23	1.364 (15)
C23-C211	1.403 (12)	C24-C25	1.300 (15)
C24-C211	1.416 (14)	C25-C212	1.479 (14)
C26-C27	1.374 (15)	C26-C212	1.416 (12)
C27-C28	1.399 (13)	C29-C210	1.428 (10)
C29-C212	1.402 (12)	C210-C211	1.439 (13)
C31-C32	1.408 (18)	C32-C33	1.351 (18)
C33-C311	1.436 (13)	C34-C35	1.350 (17)
C34-C311	1.416 (18)	C35-C312	1.387 (21)
C36-C37	1.357 (21)	C36-C312	1.391 (14)
C37-C38	1.388 (15)	C39-C310	1.431 (11)
C39-C312	1.371 (15)	C310-C311	1.414 (19)
C41-C42	1.403 (14)	C42-C43	1.428 (19)
C43-C411	1.360 (19)	C44-C45	1.251 (24)
C44-C411	1.380 (20)	C45-C412	1.486 (19)
C46-C47	1.370 (18)	C46-C412	1.359 (21)
C47-C48	1.412 (18)	C49-C410	1.435 (18)
C49-C412	1.402 (16)	C410-C411	1.388 (15)

Table III. Bond Angles (deg)

μ-O-Fe1-H$_2$O1	95.9 (3)	μ-O-Fe1-N1	95.6 (3)
H$_2$O1-Fe1-N1	165.8 (2)	μ-O-Fe1-N2	100.8 (2)
H$_2$O1-Fe1-N2	92.2 (3)	N1-Fe1-N2	77.4 (3)
μ-O-Fe1-N3	173.5 (2)	H$_2$O1-Fe1-N3	85.0 (3)
N1-Fe1-N3	84.5 (3)	N2-Fe1-N3	85.6 (2)
μ-O-Fe1-N4	97.5 (2)	H$_2$O1-Fe1-N4	95.9 (3)
N1-Fe1-N4	90.9 (3)	N2-Fe1-N4	159.1 (3)
N3-Fe1-N4	76.1 (2)	μ-O-Fe2-H$_2$O2	96.8 (2)
μ-O-Fe2-N5	102.7 (3)	H$_2$O2-Fe2-N5	90.9 (3)
μ-O-Fe2-N6	97.5 (2)	H$_2$O2-Fe2-N6	162.4 (3)
N5-Fe2-N6	76.0 (3)	μ-O-Fe2-N7	171.5 (3)
H$_2$O2-Fe2-N7	83.5 (2)	N5-Fe2-N7	85.8 (3)
N6-Fe2-N7	83.9 (3)	μ-O-Fe2-N8	96.6 (3)
H$_2$O2-Fe2-N8	98.6 (3)	N5-Fe2-N8	157.3 (3)
N6-Fe2-N8	89.8 (3)	N7-Fe2-N8	75.0 (3)
Fe1-μ-O-Fe2	155.1 (4)	Fe1-N1-C11	127.6 (7)
Fe1-N1-C110	113.9 (6)	C11-N1-C110	118.5 (9)
Fe1-N2-C18	126.7 (8)	Fe1-N2-C19	114.8 (5)
C18-N2-C19	118.5 (8)	Fe1-N3-C21	128.4 (6)
Fe1-N3-C210	112.0 (5)	C21-N3-C210	119.5 (7)
Fe1-N4-C28	124.6 (6)	Fe1-N4-C29	116.2 (4)
C28-N4-C29	119.2 (7)	Fe2-N5-C31	126.8 (8)
Fe2-N5-C310	114.3 (6)	C31-N5-C310	118.9 (10)
Fe2-N6-C38	126.4 (8)	Fe2-N6-C39	114.6 (5)
C38-N6-C39	119.0 (8)	Fe2-N7-C41	129.0 (7)
Fe2-N7-C410	113.2 (7)	C41-N7-C410	117.6 (9)
Fe2-N8-C48	123.4 (7)	Fe2-N8-C49	117.1 (8)
C48-N8-C49	119.5 (9)	N1-C11-C12	121.9 (8)
C11-C12-C13	119.0 (10)	C12-C13-C111	120.8 (13)
C15-C14-C111	120.4 (13)	C14-C15-C112	121.1 (10)
C17-C16-C112	119.9 (9)	C16-C17-C18	118.7 (10)
N2-C18-C17	122.1 (12)	N2-C19-C110	116.8 (7)
N2-C19-C112	123.5 (8)	C110-C19-C112	119.7 (11)
N1-C110-C19	116.9 (10)	N1-C110-C111	122.9 (8)
C19-C110-C111	120.2 (8)	C13-C111-C14	123.7 (12)
C13-C111-C110	116.9 (9)	C14-C111-C110	119.3 (9)
C15-C112-C16	123.5 (9)	C15-C112-C19	119.3 (9)
C16-C112-C19	117.2 (12)	N3-C21-C22	121.8 (8)
C21-C22-C23	119.9 (8)	C22-C23-C211	119.8 (9)
C25-C24-C211	122.2 (10)	C24-C25-C212	122.8 (10)
C27-C26-C212	119.7 (9)	C26-C27-C28	119.9 (8)
N4-C28-C27	122.0 (8)	N4-C29-C210	116.8 (7)
N4-C29-C212	122.0 (7)	C210-C29-C212	121.1 (8)
N3-C210-C29	118.9 (7)	N3-C210-C211	121.9 (7)
C29-C210-C211	119.1 (8)	C23-C211-C24	124.5 (9)
C23-C211-C210	117.1 (8)	C24-C211-C210	118.4 (8)
C25-C212-C26	126.5 (9)	C25-C212-C29	116.3 (8)
C26-C212-C29	117.1 (8)	N5-C31-C32	122.8 (10)
C31-C32-C33	119.1 (9)	C32-C33-C311	120.1 (13)
C35-C34-C311	120.5 (15)	C34-C35-C312	121.1 (13)
C37-C36-C312	120.6 (11)	C36-C37-C38	119.7 (9)
N6-C38-C37	120.2 (11)	N6-C39-C310	116.0 (9)
N6-C39-C312	124.1 (8)	C310-C39-C312	119.9 (11)
N5-C310-C39	119.0 (11)	N5-C310-C311	122.7 (8)
C39-C310-C311	118.3 (10)	C33-C311-C34	124.3 (13)
C33-C311-C310	116.3 (11)	C34-C311-C310	119.4 (10)
C35-C312-C36	122.8 (11)	C35-C312-C39	120.8 (9)
C36-C312-C39	116.4 (12)	N7-C41-C42	123.0 (11)
C41-C42-C43	114.1 (11)	C42-C43-C411	126.4 (11)
C45-C44-C411	119.8 (13)	C44-C45-C412	123.5 (13)
C47-C46-C412	118.8 (12)	C46-C47-C48	120.2 (13)
N8-C48-C47	120.5 (10)	N8-C49-C410	117.4 (10)
N8-C49-C412	121.5 (12)	C410-C49-C412	121.1 (10)
N7-C410-C49	117.2 (9)	N7-C410-C411	127.1 (12)
C49-C410-C411	115.7 (11)	C43-C411-C44	124.0 (11)
C43-C411-C410	111.7 (12)	C44-C411-C410	124.2 (12)
C45-C412-C46	125.1 (12)	C45-C412-C49	115.5 (13)
C46-C412-C49	119.5 (11)		

Figure 1. View of the structure of the [Fe$_2$O(phen)$_4$(H$_2$O)$_2$]$^{4+}$ cation, together with the numbering scheme used in the structural discussion. Thermal ellipsoids are shown at the 50% probability level, and hydrogen atoms have been omitted for clarity.

addition, these rings are nearly eclipsed (rotation of Fe2 by 16° about the Fe2-μ-O bond would bring phen 3 and phen 1 into the eclipsed configuration). Although the balance of factors that determine Fe-O-Fe bond angles is not well understood,[38] phen ring interactions are likely to play a significant role in the present complex.

Electronic Spectra. The electronic absorption spectrum of an aqueous solution of the nitrate salt of the [Fe$_2$O(phen)$_4$-(H$_2$O)$_2$]$^{4+}$ complex is shown in Figure 2. The only well-resolved optical maxima occur at ~225 and ~265 nm with extinction coefficients ~100 000 M^{-1} cm^{-1}. The perchlorate and chloride salts have identical spectra within the limits stated

in Figure 2. In the ligand field region, two shoulders are apparent at ~575 and ~490 nm with ϵ <350 M^{-1} cm^{-1}, which are similar in position and intensity to the $^6A_1 \rightarrow {}^4T_2(^4G)$ and $^6A_1 \rightarrow (^4A_1, {}^4E)(^4G)$ transitions, respectively, observed in other high-spin, octahedral Fe(III) complexes.[17] In addition, a well-resolved shoulder with an apparent λ_{max} ~350 nm (ϵ ~8000 M^{-1} cm^{-1}) may be noted, which has an absorption energy and intensity similar to those of O$^{2-} \rightarrow$ Fe(III)

(38) Murray, K. S. *Coord. Chem. Rev.* **1974**, *12*, 1.
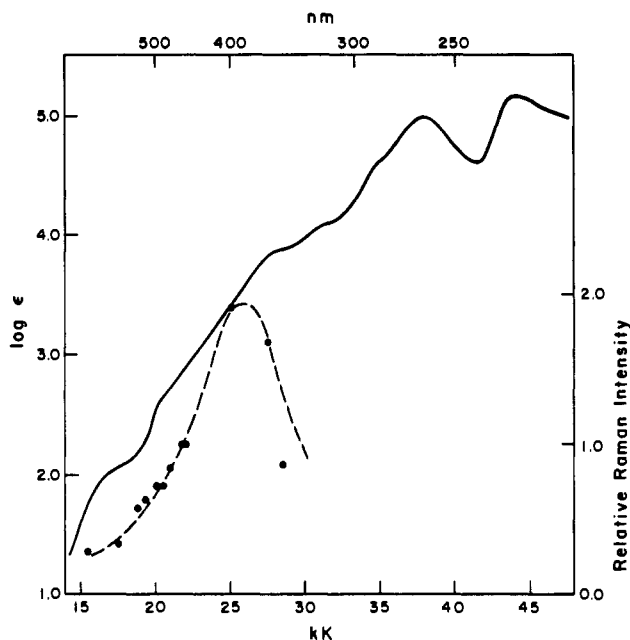
Figure 2. Electronic absorption spectrum of an aqueous solution of the $[Fe_2O(phen)_4(H_2O)_2]X_4$ complexes ($X = NO_3^-$, ClO_4^-, Cl^-). For the three salts, their ϵ and λ values coincided within 5% and 5 nm, respectively. The dashed line is the best symmetrical curve for the observed resonance enhancement of the 395-cm^{-1} line assigned to ν_s(Fe–O–Fe) for the NO_3^- salt.
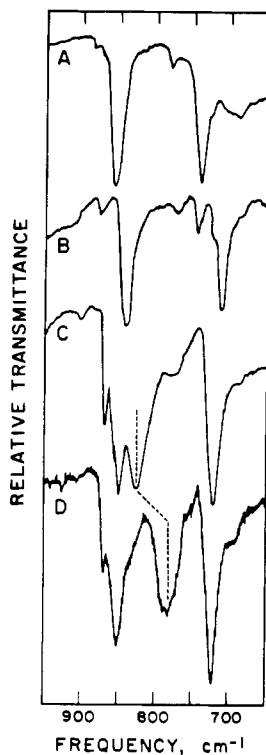
Figure 3. Infrared absorption spectra: (A) phenanthroline; (B) $[Fe(phen)_3](ClO_4)_3\cdot3H_2O$; (C) $[Fe_2O(phen)_4(H_2O)_2](NO_3)_4\cdot5H_2O$ prepared from normal isotopic abundance water; (D) the same binuclear iron complex prepared in $H_2^{18}O$. The dashed line indicates the isotope shift of the ν_{as}(Fe–O–Fe).

charge-transfer transitions assigned in hemerythrin[20] and ribonucleotide reductase.[25] The electronic spectral data shown here for aqueous solutions of the binuclear iron complexes agree well with the reflectance spectra previously reported.[39]

(39) Reiff, W. M.; Baker, W. A., Jr.; Erickson, N. E. *J. Am. Chem. Soc.* **1968**, *90*, 4794.
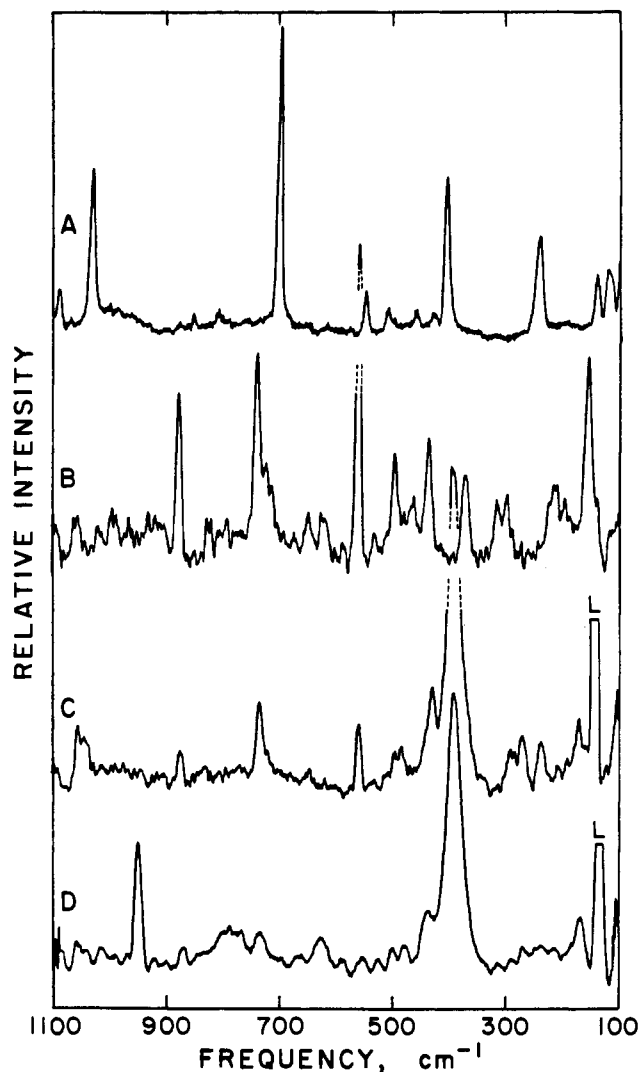
Figure 4. Raman and resonance Raman spectra: (A) phenanthroline, 457.9-nm excitation, sample at ~77 K; (B) $[Fe(phen)_3](ClO_4)_3\cdot3H_2O$, 514.5-nm excitation, ~77 K; (C) solid $[Fe_2O(phen)_4(H_2O)_2]$-$(NO_3)_4\cdot5H_2O$, with 457.9-nm excitation at ~300 K; (D) the same complex with 363.8-nm radiation but to which solid $NaClO_4$ had been added as a reference standard.

Vibrational Spectra. Infrared spectra of phenanthroline, the $[Fe(phen)_3]^{3+}$ monomer, and the nitrate salt of $[Fe_2O$-$(phen)_4(H_2O)_2]^{4+}$ are compared in Figure 3. As observed previously,[5,39] the dimer has a strong new absorption at 827 cm^{-1}, which is characteristic of the asymmetric stretch of an Fe–O–Fe moiety. Proof for this assignment was obtained by preparing the compound in $H_2^{18}O$ and finding that the corresponding vibrational mode shifts to 788 cm^{-1} (Figure 3D).

Whereas ν_{as}(M–O–M) is a dominant feature in the infrared spectra of μ-oxo-bridged binuclear metal complexes, the Raman spectra are expected to show a greater contribution from the symmetric M–O–M vibration.[39] Thus, the nitrate salt of $[Fe_2O(phen)_4(H_2O)_2]^{4+}$ exhibits a Raman spectrum whose strongest feature at 395 cm^{-1} (Figure 4C,D) is not apparent in the spectrum of either the free ligand (Figure 4A) or the tris-chelated complex of the monomer (Figure 4B). The Raman spectrum of the binuclear complex prepared in $H_2^{18}O$ shows a 5-cm^{-1} shift to lower frequency for the 395-cm^{-1} peak and is thereby identified as the ν_s(Fe–O–Fe) mode (Figure 5). There is also a smaller feature at 827 cm^{-1} that shifts to 786 cm^{-1} in $H_2^{18}O$ (Figure 5). Since these frequencies are nearly identical with those observed in the infrared spectrum of the $[Fe_2O(phen)_4(H_2O)_2]^{4+}$ nitrate complex, this weaker feature is assigned as the ν_{as}(Fe–O–Fe) mode. These data are

Table IV. Raman Frequencies in the 190–1100-cm⁻¹ Region for the [Fe₂O(phen)₄(H₂O)₂]X₄ Complexes[a]

NO₃⁻	ClO₄⁻	Cl⁻	assignment
1053 (30)	1056 (27)	1053 (15)	
1042 (25)	...	...	$\nu_1(NO_3^-)$
...	929 (16)	...	$\nu_1(ClO_4^-)$
903	909		
873 (20)	871 (16)	867 (6)	
827	828	818	$\nu_{as}(Fe-O-Fe)$
734 (45)	735 (50)	733 (30)	
646	646	640	
558 (35)	558 (38)	557 (8)	
506 (11)	505 (11)	507 (8)	
484 (12)	486 (11)	483 (11)	
		443 (11)	
430 (32)	430 (42)	427 (11)	
395 (100)	402 (100)	374 (100)	$\nu_s(Fe-O-Fe)$
313	313		
292 (9)	292 (15)	298 (9)	
	275 (8)	275 (9)	
268 (7)		262	
237	233	238	
208	192	200	

[a] Peak positions are averaged values from room-temperature spectral data obtained with visible excitation wavelengths, 457.9–647.1 nm; intensities are taken from spectra obtained with 514.5-nm excitation, for which the strong peak at ≃400 cm⁻¹ [ν_s(Fe–O–Fe)] is set to 100%; peaks with no intensities indicated are very weak (<5%) and less certain in frequencies.

analogous to an earlier Raman study of [Fe₂OCl₆]²⁻ in which both symmetric and asymmetric Fe–O–Fe modes were observed at 458 and 870 cm⁻¹, respectively, in H₂¹⁶O and at 440 and 826 cm⁻¹, respectively, in H₂¹⁸O.[29]

The Raman spectra of the perchlorate and chloride salts of [Fe₂O(phen)₄(H₂O)₂]⁴⁺ were remarkably similar to that of the nitrate salt, as can be seen from the frequency and relative intensity data collected in Table IV. Although the Raman intensities of ν_{as}(Fe–O–Fe) were also weak in the Cl⁻ and ClO₄⁻ salts, these modes were clearly observed in their respective infrared spectra. The chloride salt was crystallized from H₂¹⁸O and showed the expected infrared shift from 825 to 788 cm⁻¹ for an Fe–O–Fe vibration. In an earlier study of the chloride complex,[5] an additional new feature appeared at ~250 cm⁻¹ in the infrared spectrum and was tentatively assigned to an Fe–Cl stretching mode. We saw no indication of this peak in either our infrared or Raman spectra. In view of the spectral similarities among the three compounds (Table IV), it is likely that the complex cation has the structure shown in Figure 1 for all of the binuclear complexes we prepared.

As has been found for other oxo-bridged metal complexes,[26–28] the Raman intensity of ν_s(Fe–O–Fe) in [Fe₂O(phen)₄(H₂O)₂]⁴⁺ complexes is very sensitive to excitation wavelength. In going from 457.9 to 363.8 nm excitation (Figure 4C,D), for example, the intensity of the 395-cm⁻¹ band increases markedly relative to the other vibrational frequencies of the complex. The change in intensity may be gauged
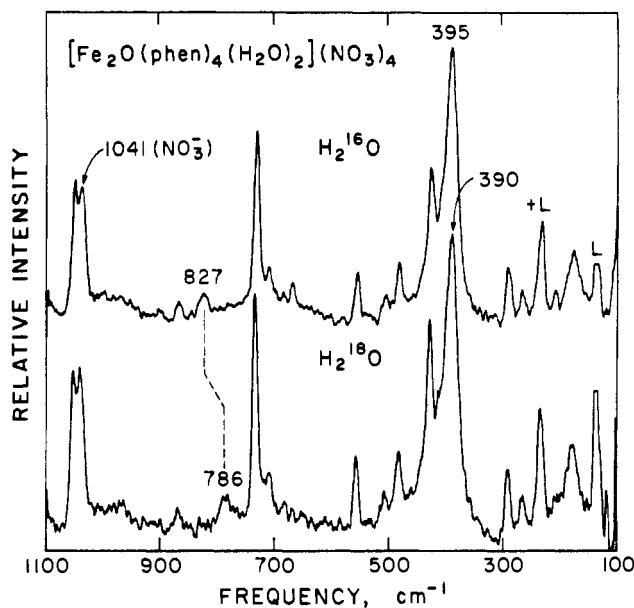
Figure 5. Raman spectra of solid [Fe₂O(phen)₄(H₂O)₂](NO₃)₄·5H₂O obtained with 647.1-nm excitation and prepared either in normal water (upper trace) or in H₂¹⁸O (lower trace). The dashed line indicates the isotope shift of the ν_{as}(Fe–O–Fe). The ν_s(Fe–O–Fe) at 395 cm⁻¹ was observed to shift to 390 cm⁻¹ in the nitrate salt.

relative to a phenanthroline mode at ~734 cm⁻¹ in the binuclear complex, which appears as a strong peak at ~700 cm⁻¹ in the free ligand (Figure 4A) and at ~740 cm⁻¹ in [Fe(phen)₃](ClO₄)₃ (Figure 4B). The change in intensity of the 395-cm⁻¹ band with excitation wavelengths was quantitated by using either the phen mode at 734 cm⁻¹ or the $\nu_1(NO_3^-)$ mode at 1041 cm⁻¹ in the spectra of the nitrate salt as the internal standard both of which gave similar values. In the near-UV and UV regions $\nu_1(ClO_4^-)$ of solid NaClO₄, which was mixed with the complex salts, was used as a standard (normalized to 457.9-nm excitation) since the phen and counterion modes were now too low in intensity to be used as reliable internal standards (see Figure 4D). The resulting resonance enhancement profile for the 395-cm⁻¹ band is also shown in Figure 2 in relation to the absorption spectrum, where the dashed line approximates the best symmetrical curve through the available data points. Similar enhancement profiles for the corresponding Fe–O–Fe vibration were exhibited by the chloride and perchlorate salts. The apparent maximum in the profile at ~380 nm suggests that this region of the electronic spectrum contains a substantial contribution from μ-oxo → Fe(III) charge transfer. The similarity of the Raman behavior of the ferric phenanthroline dimer to that of hemerythrin[20] and ribonucleotide reductase[25] suggests that resonance enhancement of the Fe–O–Fe mode in the near-ultraviolet region may be a common (although not absolute) characteristic of μ-oxo-bridged binulear iron complexes. A previous study of eight complexes known to contain the Fe–

Table V. Structural, Magnetic, and Vibrational Spectroscopic Properties of Binuclear Iron Complexes with μ-Oxo Bridging Groups

Fe(III) complex	Fe–O–Fe angle, deg	Fe–O dist, Å	Fe–Fe sepn, Å	−J, cm⁻¹	¹⁶O (¹⁸O) ν(Fe–O–Fe), cm⁻¹ asym, IR	¹⁶O (¹⁸O) ν(Fe–O–Fe), cm⁻¹ sym, Raman
μ-oxo-bridged dimers[a]	139–180	1.76–1.82	3.3–3.6	90–115	800–890	
Fe₂O(TPP)₂[b]	174.5	1.763	3.52	100–155	878[c]	363
(Hpy)₂[Fe₂OCl₆][d]	155.6	1.755	3.43		870 (826)	458 (440)
[Fe₂O(phen)₄(H₂O)₂](NO₃)₄[e]	155.1	1.785	3.49	110[f]	827 (788)	395 (390)
[Fe₂O(CH₃COO)₂(HB(pz)₃)₂][g]	123.6	1.785	3.15	121	751 (721)	528 (511)
methemerythrin[h]	135	1.68–1.92	3.21	134	750 (715)[i]	510 (496)
ribonucleotide reductase[j]				108		496 (481)

[a] References 5, 34. [b] References 26, 38, 41, 42. [c] Values are 840 (780) for oxo-bridged dimer of iron deuteroporphyrin dimethyl ester.[43] [d] References 29, 44. [e] This work. [f] Reference 5. [g] References 45, 46. [h] References 10, 19, 21. [i] Raman data.[20] [j] References 24, 25.

O–Fe structural unit failed to reveal resonance-enhanced Raman modes attributable to the Fe–O–Fe symmetric stretch using 488.0-nm excitation.[29] It is possible that this vibrational feature might have been observed in some of these complexes with excitation in the near-ultraviolet region.

Conclusion

Comparisons of structural, magnetic, and vibrational spectroscopic properties of a number of μ-oxo-bridged binuclear iron complexes are given in Table V. As has been discussed previously,[34,47] the Fe–O distances fall within a narrow range whereas the Fe–O–Fe angles (and, therefore, Fe–Fe separations) are much more variable. Furthermore, these complexes show a high degree of antiferromagnetic interaction, which appears to be a consequence of Fe–O σ bonding and is relatively unrelated to bond angle. The Fe–O–Fe vibrations, on the other hand, do appear to correlate with bond angle as has been delineated by Wing and Callahan[40] for oxo-bridged complexes of molybdenum. The general trend of ν_{as}(Fe–O–Fe) to decrease with decreasing bond angle and of ν_s(Fe–O–Fe) to increase with decreasing bond angle is borne out by the iron complexes in Table V. The $^{16}O \rightarrow {}^{18}O$ frequency shifts of 5–18 cm^{-1} for ν_s(Fe–O–Fe) and 40–60 cm^{-1} for ν_{as}(Fe–O–Fe) are also within the ranges expected for these bridged structures.[40]

(40) Wing, R. M.; Callahan, K. P. *Inorg. Chem.* **1969**, *8*, 871.
(41) Hoffman, A. B.; Collins, D. M.; Day, V. W.; Fleischer, E. B.; Srivastava, T. S.; Hoard, J. L. *J. Am. Chem. Soc.* **1972**, *94*, 3620.
(42) Fleischer, E. B.; Srivastava, T. S. *J. Am. Chem. Soc.* **1969**, *91*, 2403.
(43) Sadisivan, N.; Eberspaecher, H. I.; Fuchsman, W. H.; Caughey, W. S. *Biochemistry* **1969**, *8*, 534.
(44) Drew, M. G. B.; McKee, V.; Nelson, S. M. *J. Chem. Soc., Dalton Trans.* **1978**, 80.
(45) Armstrong, W. H.; Lippard, S. J. *J. Am. Chem. Soc.* **1983**, *105*, 4837.
(46) Armstrong, W. H.; Spool, A.; Papaefthymiou, G. C.; Frankel, R. B.; Lippard, S. J. *J. Am. Chem. Soc.* **1984**, *106*, 3653.
(47) Mabbs, F. E.; McLachlan, V. N.; McFadden, D.; McPhail, A. T. *J. Chem. Soc., Dalton Trans.* **1973**, 2016.

The singly bridged μ-oxo dimers have long been considered as good models for the electronic and magnetic properties of binuclear iron proteins such as hemerythrin and ribonucleotide reductase. The work reported here indicates that these complexes are also appropriate models for the resonance Raman spectroscopic properties of these binuclear iron proteins. Although the iron complex in hemerythrin contains two carboxylate bridges in addition to a μ-oxo bridge,[10–12] its spectroscopic and magnetic characteristics appear to be dominated by the Fe–O–Fe component. This is further supported by work on the recently described binuclear iron complex [Fe$_2$O-(CH$_3$COO)$_2$(HB(pz)$_3$)$_2$],[45] in which the irons share three bridging groups, a μ-oxo and two bidentate carboxylates, as in hemerythrin. The vibrational spectroscopic values of the triply bridged complex (Table V) are in the range expected for an Fe–O–Fe species with a bridging angle of 124°.

Registry No. [Fe$_2$O(phen)$_4$(H$_2$O)$_2$]Cl$_4$, 92282-00-3; [Fe$_2$O-(phen)$_4$(H$_2$O)$_2$](NO$_3$)$_4$·5H$_2$O, 92282-02-5; [Fe$_2$O(phen)$_4$(H$_2$O)$_2$]-(ClO$_4$)$_4$, 92217-00-0; Fe(phen)$_3$(ClO$_4$)$_3$, 14634-90-3; ^{18}O, 14797-71-8.

Supplementary Material Available: Tables of anisotropic thermal parameters, calculated coordinates and *U*'s for hydrogen atoms, metric parameters for unconstrained nitrate groups, site occupancy factors, and structure factors (38 pages). Ordering information is given on any current masthead page.

Contribution from the Department of Chemistry,
Texas Christian University, Fort Worth, Texas 76129

Iron Porphyrin Models of Peroxidase Enzyme Intermediates: Oxidation of Deuteroferriheme by C₆H₅IO and C₆H₅I(OAc)₂

HENRY C. KELLY* and SRITANA C. YASUI

Treatment of the iron(III) complex of deuteroporphyrin IX, deuteroferriheme, with iodosobenzene or (diacetoxyiodo)benzene (commonly called iodobenzene diacetate) yields an oxidized form of the iron porphyrin which is spectrally identical to that obtained from heme oxidation by peroxo substrates and chlorite ion and which mimics the catalytic activity of reaction intermediates derived from hemoprotein peroxidase enzymes. Two moles of iron porphyrin is stoichiometrically equivalent to 1 mol of oxidant, suggesting the heme-derived "intermediate state" to consist of one or more one-electron oxidation products of heme iron(III). Stopped-flow spectrophotometric determination of the rate of intermediate formation shows a first-order dependence on both *monomeric* heme and oxidant, the second-order rate constant for oxidation by iodobenzene diacetate being about twice that obtained with iodosobenzene. This is tentatively attributed to a statistical factor associated with O-atom donation of C₆H₅I-bound oxygen to the iron(III) center. Regeneration of free heme from "intermediate state" is dependent on the nature and concentration of oxidant and is suggested to involve catalytic turnover of oxidant analogous to heme-catalyzed decomposition of H₂O₂.

Introduction

Numerous studies of the peroxidase-like catalytic activity of iron(III) porphyrins (hemes) have focused on the oxidative formation and reactivity of intermediate species that appear to be functional analogues of intermediates generated in hemoprotein enzyme systems.[1–11] Such studies are somewhat

complicated by the tendency of the protein-free hemes to aggregate in aqueous solution,[12–14] since it is the nonaggregated

(1) Portsmouth, D.; Beal, E. A. *Eur. J. Biochem.* **1971**, *19*, 479.

(2) Jones, P.; Prudhoe, K.; Robson, T.; Kelly, H. C. *Biochemistry* **1974**, *13*, 4279.
(3) Kelly, H. C.; Davies, D. M.; King, M. J.; Jones, P. *Biochemistry* **1977**, *16*, 3543.
(4) Jones, P.; Mantle, D.; Davies, D. M.; Kelly, H. C. *Biochemistry* **1977**, *16*, 3974.
(5) Jones, P.; Mantle, D. *J. Chem. Soc., Dalton Trans.* **1977**, 1849.